

Quadric surface projection model for fish-eye cameras

Tiantian Meng (孟甜甜)^{1*}, Jintao Jiang (蒋金涛)², and Ming Yang (杨鸣)³

¹Faculty of Information Science and Engineering, Ningbo University, Ningbo 315211, China

²Zhejiang High-tech Medical Optoelectronic Equipment Research and Development Center, Ningbo University, Ningbo 315211, China

*Corresponding author: tpmengt@126.com

Received April 19, 2011; accepted June 10, 2011; posted online August 30, 2011

The curved surface projection model in fisheye image correction algorithm is presented. To analyze the causes of distortion in existing models, we establish an ideal surface projection model and compare its surface with the surfaces of existing models. Subsequently, feature points are obtained on the ideal surface according to the relationship of coordinates of fish-eye image points and their ideal three-dimensional (3D) points. Finally, the least square method is used to obtain a quadric surface and presents a quadric surface projection model. The experiment shows that the corrected image of the new model is more similar to the actual scene than the corrected images of previous models.

OCIS codes: 100.3008, 100.3010, 140.1135, 140.1488.

doi: 10.3788/COL201210.011002.

Fish-eye lenses have extremely short focal length and a very wide field of view (FOV), which is generally close to 180° or even wider^[1]. One single fish-eye image can represent a large part of the surroundings. Thus, use of fish-eye lens in detection and survey systems has attracted considerable attention. Wu *et al.*^[2,3] have used fish-eye lens in automatic surveillance.

In order to obtain a large FOV, a fish-eye lens uses the “non-similar” imaging thought. As a result, considerable barrel distortion in fish-eye images occurs. In recent years, fish-eye algorithm has been extensively studied. However, fish-eye lens optical transformation is complex and different fish-eye lens have different designs. Hughes *et al.*^[4,5] have evaluated several fish-eye algorithms and found that one algorithm could not fit all types of fish-eye lenses. However, previous work did not address fish-eye lenses with FOV beyond 180°. In this letter, a circular fish-eye lens with a FOV of 186° is used. We adopt the surface projection model to derive the coordinate transformation between the fish-eye image points and their matching scene three-dimensional (3D) points by orthogonal projection. Spherical projection model is used in most applications^[6–9]. However, for orthogonal projection, the spherical projection model inherently limits the FOV of the camera to 180°. When the spherical projection model is used to correct the 186° fish-eye lens, the corrected image is marked with barrel distortion. The parabolic projection model proposed by Wang *et al.* does not have limitations of the spherical projection^[10]. However, several pincushion distortions exist in the corrected image of the parabolic projection.

According to the imaging theory of fish-eye lens, the surface projection model can simulate the optical transformation process. The corresponding relationship between the target points and the fish-eye image points can be determined by the model, and the fish-eye images can be corrected and transformed to normal plane perspective images.

The rules of fish-eye surface projection model are shown in Fig. 1. Suppose that the camera is at the origin of coordinate O , shooting along the Z axis direc-

tion. The image taken by fish-eye lens is at the OXY plane and fills a circular area. O is the center of the fish-eye image outline and R is the radius. P_1 and P_2 are the two points on the spatial line. P_{s1} and P_{s2} are the two crossing points of OP_1 ray and OP_2 ray in relation to the surface. Drawing lines perpendicular to the OXY plane through the two points, we can obtain points P_{t1} and P_{t2} . P_{t1} and P_{t2} are the corresponding points in the fish-eye imaging planes of P_1 and P_2 after the transformation of fish-eye lens. Straight lines are transformed to curved lines by the fish-eye lens. The space coordinates of P_1 are (X, Y, Z) , the coordinates of P_{t1} on the imaging plane are (u, v) , and the centers of the fish-eye image outline O are (u_0, v_0) . Consequently, the corresponding relationship between the target points and the fish-eye image points can be expressed as

$$(u - v_0, v - v_0) = D(X, Y, Z), \quad (1)$$

where $D(X, Y, Z)$ represents the correction formula.

Previous studies have used the spherical projection model to correct fish-eye images^[3–6]. The projection surface equation is expressed as

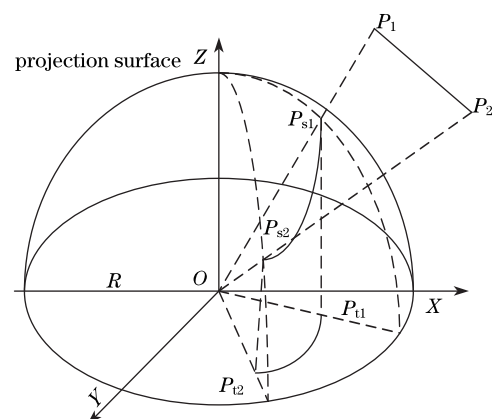


Fig. 1. Rules of fish-eye surface projection model.

$$x^2 + y^2 + z^2 = R^2. \tag{2}$$

The correction formula $D(X, Y, Z)$ is

$$\begin{aligned} (u - u_0) &= \frac{R}{\sqrt{X^2 + Y^2 + Z^2}} X \\ (v - v_0) &= \frac{R}{\sqrt{X^2 + Y^2 + Z^2}} Y \end{aligned} \tag{3}$$

Sphere can be seen as the rotation surface around the Z axis, and thus the generatrix of the surface is

$$x^2 + z^2 = R^2. \tag{4}$$

Earlier studies have used the parabolic projection model to correct fish-eye image^[6]. The projection surface equation is expressed as

$$z = \frac{R^2 - (x^2 + y^2)}{2R}. \tag{5}$$

The correction formula $D(X, Y, Z)$ is

$$\begin{aligned} (u - u_0) &= R \frac{\sqrt{Z^2 + X^2 + Y^2} - Z}{X^2 + Y^2} X \\ (v - v_0) &= R \frac{\sqrt{Z^2 + X^2 + Y^2} - Z}{X^2 + Y^2} Y \end{aligned} \tag{6}$$

The generatrix of the parabolic surface is

$$z = \frac{R^2 - x^2}{2R}. \tag{7}$$

The aim of fish-eye image correction is to restore the realistic situations; the straight lines in the captured real scene must also be straight in the corrected image. Each point on the fish-eye image has an ideal corresponding point on the calibration target plane and their relationship can be identified by establishing the ideal projection surface model.

The ideal surface projection model is shown in Fig. 2. Suppose that the calibration target plane parallel is the imaging plane with a distance of R , the center of the target plane O' is at $(0, 0, R)$, and P is the ideal corresponding point of I in the calibration target plane; an ideal projection surface exists between the calibration target plane and the imaging plane, which has a crossing point P_s with ray OP . P_s represents the feature points on the ideal projection surface. For every point of the fish-eye image, there is a corresponding P_s on the projection surface. The surface composition of these points is the ideal fish-eye projection surface.

If the coordinates of P are (X, Y, Z) , the coordinates of I in the image plane coordinate system are (u, v) , and the fish-eye image center is $O(u_0, v_0)$, then the coordinates of P_s can be obtained by

$$\left(x, y, \frac{\sqrt{x^2 + y^2}}{\sqrt{X^2 + Y^2}} Z \right), \tag{8}$$

where $x = u - u_0, y = v - v_0$

When the coordinates of the fish-eye image feature point P and its ideal corresponding point I are known,

we can derive the feature points of and fit the ideal projection surface.

The projection surface is a revolving surface, hence, the difference between the ideal surface and the surfaces of the existing model can be obtained by extracting the feature points on the generatrix of the ideal projection surface. Figure 3 is a fish-eye grid image taken by a 0.33-mm fish-eye lens with a FOV of 186°. The specific steps of the feature point extraction on the generatrix are detailed below.

Firstly, the radius R and the center coordinates (u_0, v_0) are determined. The circular fish-eye lens obtains a profile of its circular effective area; therefore scan line approximation algorithm can be adopted to derive the parameters. The brightness difference threshold is set and the image is scanned from the four sides to the center. The brightness of each point in each scan line is computed to determine the maximum brightness I_{\max} and minimum brightness I_{\min} . The ultimate difference of brightness of the scan line I_{lim} is

$$I_{\text{lim}} = I_{\max} - I_{\min}. \tag{9}$$

If I_{lim} is greater than the threshold, the scan line reaches the edge of circular effective area. Thus, the center coordinates of the circle and the radius can be decided.

Secondly, the net points $I_i (i = 1, 2, \dots, n)$ intersecting with the X -axis are selected as the feature points in the fish-eye image and $(x_i, 0, 0)$ are designated as their coordinates, similar to the star points shown in Fig. 3. The distortion in the center of fish-eye lens is slight, thus the ideal imaging grid spacing d can use the grid spacing near the center of the fish-eye image. The actual scene is an equally spaced grid, and the ideal corresponding points P_i are marked as $(X_i, 0, R)$, where x_i can be expressed

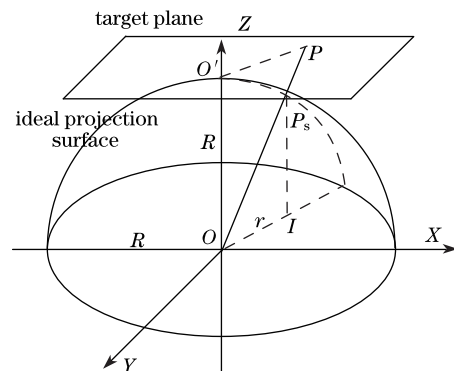


Fig. 2. Ideal projection model surface.

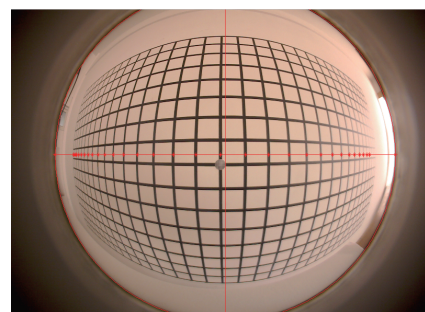


Fig. 3. Grid image taken by fish-eye lens.

as

$$X_i = x_i + (i - 1)d. \tag{10}$$

Finally, Eq. (8) is used to obtain the coordinate of the feature points P_{si} on the generatrix of the ideal surface.

In Fig. 4, the star points are represented by P_{si} , the dashed line is the generatrix of the spherical model, and the dash dotted line is the generatrix of the parabolic model. The feature points are not close to the spherical or parabolic curve but distributed between the two curves. Using the different models, the same point on the target plane obtains two different points. As the distance of one point from the center goes farther than the ideal point, the other point gets nearer. These results explain the barrel distortion in the spherical model and the pincushion distortion in the paraboloid model.

In this letter, we fit the feature points to obtain a quadric surface as the projection surface and propose the quadric surface projection model. A rotational quadric surface around the Z -axis is established, and thus the general quadric equation can be set as

$$A(x^2 + y^2) + B(\sqrt{x^2 + y^2})z + Cz^2 + D(\sqrt{x^2 + y^2}) + Ez - R^2 = 0, \tag{11}$$

where A, B, C, D, E are the quadric equation parameters that need to be fitted.

The surface and the image plane intersect at a circle whose radius is R and center at the origin. Thus

$$D = 0, \tag{12}$$

$$\sqrt{-\frac{G}{A}} = R^2.$$

After the process of simplification, Eq. (11) becomes

$$(x^2 + y^2) + B(\sqrt{x^2 + y^2})z + Cz^2 + Ez - R^2 = 0, \tag{13}$$

where three unknown parameters $B, C,$ and E can be gotten by the least squares fitting the feature points of the generatrix. The correction formula $D(X, Y, Z)$ is expressed as

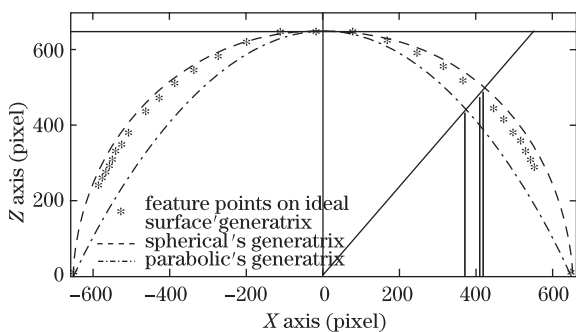


Fig. 4. Comparison of the feature points and the generatrix of models.

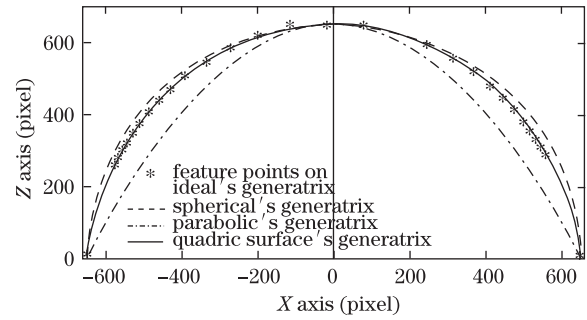


Fig. 5. Quadric surface fitting results.

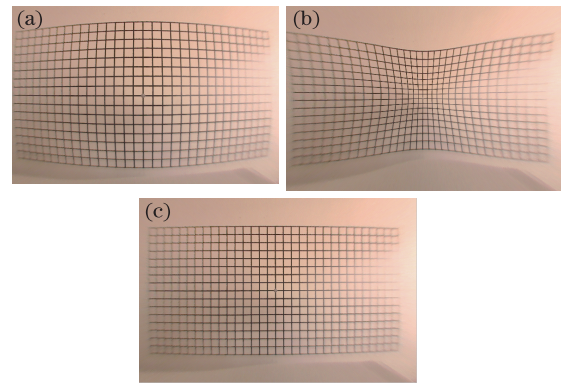


Fig. 6. Corrected images using (a) spherical model, (b) parabolic model, and (c) quadric model.

$$(u - u_0) = \frac{\sqrt{EZ^2 + 4(X^2 + Y^2)R} - EZ}{2(X^2 + Y^2 + BZ\sqrt{X^2 + Y^2} + CZ)}X$$

$$(v - v_0) = \frac{\sqrt{EZ^2 + 4(X^2 + Y^2)R} - EZ}{2(X^2 + Y^2 + BZ\sqrt{X^2 + Y^2} + CZ)}Y \tag{14}$$

Feature point fitting has obtained the unknown parameters $B = 0.0212, C = 0.7676,$ and $D = 151.0598$. The fitting surface becomes close to the feature points of the ideal surface (Fig. 5).

To verify the effectiveness of the method, we correct Fig. 4 by spherical, parabolic, and quadric surface projection models. The sizes of corrected images are 600×400 pixels and the horizontal view angle is approximately 150° . When the angle is greater than a certain level, the spherical model causes barrel distortion (Fig. 6(a)) and the parabolic model produces obvious pincushion distortion (Fig. 6(b)) in the corrected images. Figure 6(c) shows the corrected image of the quadric projection model. Grid lines in this corrected image have become almost straight and no obvious barrel or pincushion distortion is observed. The comparison of the calibration results of these models clearly demonstrate that the quadric model is capable of correcting the barrel distortion of the fish-eye image.

In conclusion, we conduct a systemic research on the surface projection model in fish-eye image correction algorithm. In order to correct the fish eye image and make it more similar to the captured real scene, a quadric surface projection model by extracting feature points in the generatrix of the ideal surface is presented and the

corresponding correction formula is provided. The new model can be used to correct fish-eye images with very wide FOV, even those beyond 180° . The corrected image produced by the new model is very similar to the actual scene. However, a small amount of distortion in Fig. 6(c) remained, because the calibration template is not completely parallel to the image plane. Thus, it produces several errors when the coordinates of the 3D points of feature points are being determined. In future work, the rotation and translation will be considered to eliminate the effects of the action.

References

1. D. Schneider, E. Schwalbe, and H.-G. Maas, *ISPRS J. Photogrammetry Remote Sens.* **64**, 259 (2009).
2. J. Wu, K. Yang, Q. Xiang, and N. Zhang, *Chin. Opt. Lett.* **7**, 142 (2009).
3. X. Yuan, Y. Song, and X. Wei, *Chin. Opt. Lett.* **9**, 021101 (2011).
4. C. Hughes, P. Denny, E. Jones, and M. Glavin, *Appl. Opt.* **49**, 3338 (2010).
5. C. Ricolfe-Viala and A.-J. Sanchez-Salmeron, *Appl. Opt.* **49**, 5914 (2010).
6. T. N. Mundhenk, M. J. Rivett, X. Liao, and E. L. Hall, in *Proceedings of the SPIE Intelligent Robotics and Computer Vision Conference XIX* 181 (2000).
7. H. Zhao and J. K. Aggarwal, in *Proceedings of the 4th IEEE Southwest Symposium on Image Analysis and Interpretation* 219 (2000).
8. M. Kedzierski and A. Fryskowska, in *Proceedings of the International Archives of the Photogrammetry, Remote Sensing and Spatial Information Sciences* 765 (2008).
9. Gyeong-II Kweon, *J. Opt. Soc. Korea* **14**, 109 (2010).
10. J. Wang, X. Yang, and C. Zhang, *J. System Simulation* **13**, 66 (2001).